Smart Structures and Systems, Vol. 8, No. 5 (2011) 487-499
DOI: http://dx.doi.org/10.12989/sss.2011.8.5.487

Parametric resonance of axisymmetric sandwich annular plate with ER core layer and constraining layer

Jia-Yi Yeh*

Department of Information Management, Chung Hwa University of Medical Technology, 89, Wen-Hwa 1st ST. Jen-Te Hsiang, Tainan Hsien 717, Taiwan, R.O.C.

(Received January 3, 2011, Revised June 30, 2011, Accepted September 1, 2011)

Abstract. The parametric resonance problems of axisymmetric sandwich annular plate with an electrorheological (ER) fluid core and constraining layer are investigated. The annular plate is covered an electrorheological fluid core layer and a constraining layer to improve the stability of the system. The discrete layer annular finite element and the harmonic balance method are adopted to calculate the boundary of instability regions for the sandwich annular plate system. Besides, the rheological property of an electrorheological material, such as viscosity, plasticity, and elasticity can be changed when applying an electric field. When the electric field is applied on the sandwich structure, the damping of the sandwich system is more effective. Thus, variations of the instability regions for the sandwich annular plate with different applying electric fields, thickness of ER layer, and some designed parameters are presented and discussed in this study. The ER fluid core is found to have a significant effect on the location of the boundaries of the instability regions.

Keywords: parametric resonance; dynamic instability; electrorheological; annular plate; discrete layer annular finite element.

1. Introduction

When structures are subjected to periodic loads, the ordinary forced response will lead to dynamic instability of the system under some circumstances. The instability may occur under periodic loads over a range of excitation frequency. The induced violent vibration is called the parametric resonance or dynamic instability. The dynamic characteristics analyses of the plate structures had been widely investigated in mechanical applications. A number of investigators had studied the parametric resonance due to the periodic in-plane loads and two of these are Bolotin (1964) and Evan-Iwanowski (1976).

Many researchers had studied the dynamic instability of single circular and annular plates due to periodic in-plane stress systems. Tani and Nakanura (1980) investigated the dynamic stability of thin annular plate under pulsating torsion by employing the Galerkin method. Then, the parametric resonance analysis of polar orthotropic annular plate was discussed by Tani and Doki (1982). Chen and Hwang (1988) adopted the finite element and Galerkin methods to study the axisymmetric dynamic stability of isotropic and polar orthotropic thick circular plates. Then, the dynamic stability behaviors of the viscoelastic column subjected to the harmonic axial load were presented by Stevens

*Corresponding Author, Associate professor, E-mail: yeh@mail.hwai.edu.tw

(1966). And, Stevens (1969) discussed the influence of initial curvature on the dynamic stability behaviors of the viscoelastic structures based on the complex modulus representation. The parametric resonance characteristics of the non-linear viscoelastic plate are studied by Touati and Cederbaum (1994). Afterwards, Ilyasov and Akoz (2000) presented the vibration and dynamic stability of viscoelastic plates with isotropic viscoelastic constitutive relation. Chen and Chen (2004) adopted the finite element method to studied parametric resonance problems of the annular plate system with constraining damping layer.

Regarding the active control of the structural vibration to the use of the ER materials, the wide introduction about the applications of the ER material was presented by Weiss *et al.* (1993). The ER fluid has the similar properties as a viscoelastic material at small strain level and the studies for the construction of smart components had been investigated by Coulter (1993). The vibration behaviors of the sandwich beam with ER fluid core and the variations of the modal loss factors with different designed parameters of the sandwich system were calculated and discussed by Yalcintas and Coulter (1995). After that, Oyadiji (1996) presented that the modal parameters were more dependent on the location and also discussed the effects of the size of the ER fluid treatment for an aluminum plate. Kang *et al.* (2001) studied the passive and active damping characteristics of the ER composite beams and, the flexural vibration of laminated composite ER sandwich beams to maximize the possible damping capacity was also calculated in this study.

In the present study, the parametric resonance behaviors and damping properties of sandwich annular plate with an ER fluid core and constraining layer are studied. No prior work has addressed the parametric resonance problem of the sandwich annular plate with ER fluid core layer to the author's knowledge. The shear modulus of the linear isotropic ER fluid material is described by complex quantities. Besides, the discrete layer annular finite element and the harmonic balance method are adopted to calculate and obtain the instability regions of the sandwich annular plate system. Additionally, some significant effects on the dynamic behaviors of the sandwich annular plate with ER core treatment can be found in this study. The effects of the ER layer, applying electric fields and some designed parameters on the instability regions for the sandwich annular plate system are also investigated and discussed in this paper.

2. Problem formulation

The sandwich annular plate with ER core layer and constraining layer subjected to the uniform radial stress is demonstrated in Fig. 1. The base annular plate is assumed to be undamped, isotropic and designated as layer 3 with an inner radius a and outer radius b. The ER fluid core layer is designed as layer 2 and the material property of the ER material can be changed and controlled by applied different electric fields. Layer 1 is a pure elastic, isotropic constraining layer. The thicknesses of the three layers for the sandwich system are h_1, h_2, and h_3, respectively.

The following assumptions should be mentioned to simplify present problems. It is assumed that there are no slipping between the elastic and ER layers. And, the transverse displacements, w, of all points on any cross-section of the sandwich annular plate are constant. Considering the geometry of the sandwich annular plate as shown in Fig. 1, the strain-displacement relation of the elastic layer can be expressed in terms of the in-plane displacements of the adjacent layer interfaces and the transverse displacement as follows

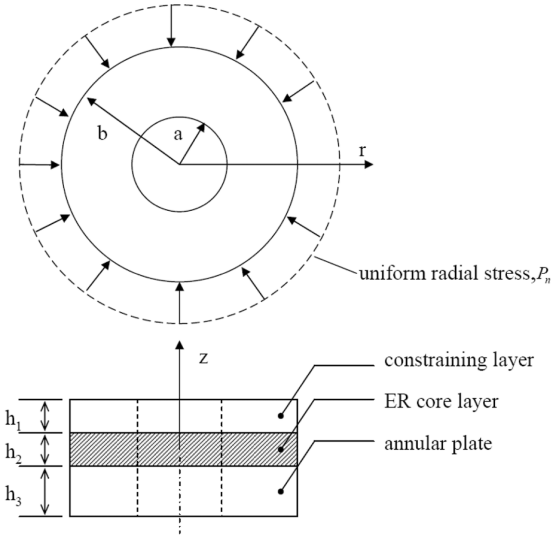

Fig. 1 Sandwich annular plate with ER layer and constraining layer treatment and subjected to the uniform radial stress

$$d_i = \begin{Bmatrix} u_i(r,z,t) \\ w_i(r,z,t) \end{Bmatrix} = H_{1,i}(z) \begin{Bmatrix} U_i(r,t) \\ U_{i+1}(r,t) \\ W(r,t) \end{Bmatrix} \tag{1}$$

in which, $H_{1,i}(z)$ is the transverse thickness interpolation matrix for *i*th layer. The discrete layer annular finite element is adopted to formulate the problem as shown in Fig. 2. Then, the displacements of the interfaces for two-layer can be shown in terms of the nodal degrees of freedom as following equation by using the interpolation in *r*-direction and the circumferential wave number *m*

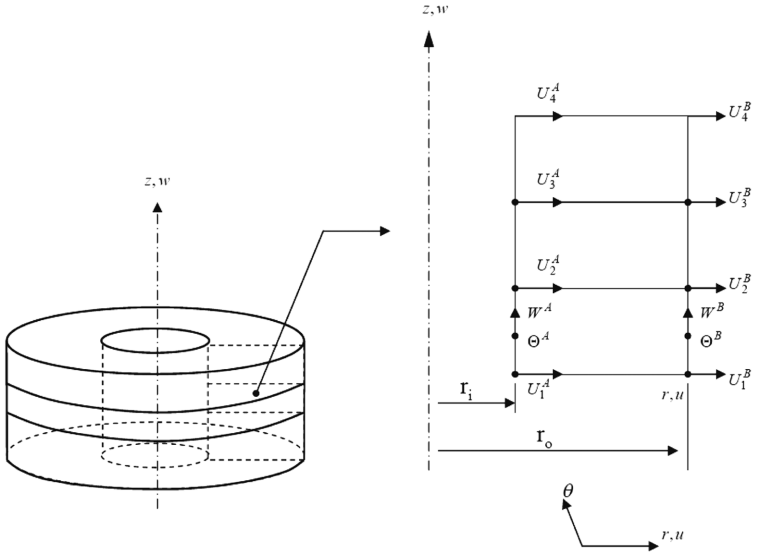

Fig. 2 The discrete layer annular finite element for three-layer element

$$\begin{Bmatrix} U_i(r,t) \\ U_{i+1}(r,t) \\ W(r,t) \end{Bmatrix} = H_2(r) q_i^e(t) \tag{2}$$

where $q_i^e(t)$ is the vector of the nodal displacements of the element, and $H_2(r)$ is the interpolation matrix.

Then, the strain-displacement relation for the ith layer of the system can be expressed as follows

$$\varepsilon_i = \begin{Bmatrix} \varepsilon_{r,i} \\ \varepsilon_{\theta,i} \\ \gamma_{rz,i} \end{Bmatrix} = Dd_i \tag{3}$$

where ε_i is the strain vector and D is the differential operator matrix.

The stress-strain relation can be obtained as the following equation

$$\sigma_i = C_i \varepsilon_i \tag{4}$$

where $\sigma_i = \{\sigma_{r,i}, \sigma_{\theta,i}, \tau_{r\theta,i}\}^T$, C_i is the elasticity matrix, respectively.

Afterwards, the strain and kinetic energies of the element for ith layer can be expressed as

$$V_i^e = \frac{1}{2}\int_V \sigma_i^T \varepsilon_i dV + \int_V \bar{\sigma}_i^T \bar{\varepsilon}_i dV \tag{5a}$$

$$T_i^e = \frac{1}{2}\int_V \rho_i \dot{u}_i^T \dot{u}_i dV \tag{5b}$$

in which, $\bar{\sigma}_i$, $\bar{\varepsilon}_i$, and ρ_i are external load stress vector, non-linear strain vector, and the mass density of the ith layer, respectively. The second term in Eq. (5(a)) is the additional strain energy due to external in-plane loads.

By substituting Eqs. (1)-(4) into Eqs. (5(a) and (b)) and adopting the Hamilton's principal, the element differential equation can be express as the following form

$$\mathrm{M}_i^e \ddot{\mathrm{U}}_i^e + (\mathrm{K}_i^e + \mathrm{G}_i^e)\mathrm{U}_i^e = 0 \tag{6}$$

in which, M_i^e, K_i^e, and G_i^e are element mass matrix, element stiffness matrix, and element geometric stiffness matrix due to the external in-plane load, respectively.

The following relations must be obtained first before combining the elemental matrices into the global stiffness and mass matrices

$$\mathrm{U}_i^e = \mathrm{Tr}_i^e \mathrm{U} \tag{7}$$

where U and Tr_i^e are the global nodal co-ordinate vector and transformation matrix.

Then, the equation of motion for the sandwich system can be express as follows by assembling the contribution of all elements of the system

$$\mathrm{M}\ddot{\mathrm{U}} + (\mathrm{K} + \mathrm{G})\mathrm{U} = 0 \tag{8}$$

where the global mass matrix M, global stiffness matrix K, and global geometric stiffness matrix G due to the external in-plane load and are given by

$$\mathrm{M} = \sum_{i=1}^{3}\left(\sum_{e=1}^{N_i} \mathrm{Tr}_i^{e^{\mathrm{T}}} \mathrm{M}_i^e \mathrm{Tr}_i^e\right) \tag{9a}$$

$$\mathrm{K} = \sum_{i=1}^{3}\left(\sum_{e=1}^{N_i} \mathrm{Tr}_i^{e^{\mathrm{T}}} \mathrm{K}_i^e \mathrm{Tr}_i^e\right) \tag{9b}$$

$$\mathrm{G} = \sum_{i=1}^{3}\left(\sum_{e=1}^{N_i} \mathrm{Tr}_i^{e^{\mathrm{T}}} \mathrm{G}_i^e \mathrm{Tr}_i^e\right) \tag{9c}$$

in which, N_i is the element number of the ith layer.

Afterwards, the external load stress, $P(t)$, is assumed to be a periodic radial stress

$$P(t) = P_0 + P_t\cos\Theta t \tag{10}$$

where P_0, P_t, and Θ are static load factor, dynamic load factor, and the disturbance frequency, respectively. Additionally, the geometric stiffness matrix can be rewritten as follows

$$\mathrm{G} = \mathrm{G}_0 + \mathrm{G}_t\cos\Theta t \tag{11}$$

where G_0 and G_t are the static geometric stiffness matrix and dynamic geometric stiffness matrix, respectively. By substituting Eq. (11) into Eq. (8), the following form called Mathieu-Hill equation can be obtained

$$\mathrm{M}\ddot{\mathrm{U}} + (\mathrm{K} + \mathrm{G}_0 + \mathrm{G}_t\cos\Theta t) + \mathrm{U} = 0 \tag{12}$$

In this section, the boundary of the dynamic instability can be calculated by using Bolotin's method (1964). And, the dynamic instability regions of the sandwich system are formed according to the periodic solutions of the T ($T = 2\pi/\Theta$) and $2T$. The boundary of the primary instability region with period $2T$ is of practical important in mechanical applications and the solution can be expressed as follows

$$\mathrm{U}(t) = \sum_{k=1,3,5,\ldots}^{\infty}\left[\{a\}_k \sin\frac{k\Theta t}{2} + \{b\}_k \cos\frac{k\Theta t}{2}\right] \tag{13}$$

where $\{a\}_k$ and $\{b\}_k$ are undetermined constants.

Substituting Eq. (13) into Eq. (12), it leads to a series of algebraic equation for the determination of the instability regions. In this study, the principle instability region, which corresponds to $k = 1$ and the instability equation for primary instability region can be presented as

$$\left(-\frac{\Theta^2}{4}\mathrm{M}+\mathrm{K}+\mathrm{G}_0-\frac{\mathrm{G}_t}{2}\right)\{a\}\sin\frac{\Theta t}{2} = \{0\} \tag{14a}$$

$$\left(-\frac{\Theta^2}{4}\mathrm{M}+\mathrm{K}+\mathrm{G}_0+\frac{\mathrm{G}_t}{2}\right)\{b\}\cos\frac{\Theta t}{2} = \{0\} \tag{14b}$$

where $\sin\left(\frac{\Theta t}{2}\right)$ and $\cos\left(\frac{\Theta t}{2}\right)$ can be expressed as exponential form and can be rewritten as follows

$$\sin\left(\frac{\Theta t}{2}\right) = \frac{-j[\exp(j\Theta t)-\exp(-j\Theta t)]}{2} \tag{15a}$$

$$\cos\left(\frac{\Theta t}{2}\right) = \frac{-j[\exp(j\Theta t)-\exp(-j\Theta t)]}{2} \tag{15b}$$

Then, substituting Eqs. (15(a) and (b)) into Eqs. (14(a) and (b)) and rewriting the equations, the following non-trivial solution of the sandwich annular plate system can be obtained

$$\begin{vmatrix} -\frac{\Theta^2}{4}\mathrm{M}+\mathrm{K}^r+\mathrm{G}_0^r-\frac{\mathrm{G}_t^r}{2} & -\mathrm{K}^j+\mathrm{G}_0^j-\frac{\mathrm{G}_t^j}{2} \\ \mathrm{K}^j+\mathrm{G}_0^j-\frac{\mathrm{G}_t^j}{2} & -\frac{\Theta^2}{4}\mathrm{M}+\mathrm{K}^r+\mathrm{G}_0^r-\frac{\mathrm{G}_t^r}{2} \end{vmatrix} = 0 \tag{16}$$

where the superscripts r and j denote the real and imaginary part of the matrices, respectively. The stability-instability boundaries of the sandwich annular system with ER core layer can be obtained by solving the above equation.

3. Numerical results and discussions

The parametric resonance analysis of the sandwich annular plate with ER fluid core and constraining layer are presented. In order to validate present algorithm and calculations obtained in this study, the numerical results are compared with those results in Roy and Ganesan (1993) and listed in Table 1. The numerical solutions solved by present model are shown to have a good agreement and accuracy. Afterwards, for convenience, the following non-dimensional parameters and some geometrical parameters are introduced

$$b=0.15m,\ \tilde{a}=\frac{a}{b},\ E_1=E_3=70GPa,\ \upsilon_1=\upsilon_3=0.29,\ \upsilon_2=0.49,\ \rho_1=\rho_3=2700kg/m^3,\ \rho_2=1700kg/m^3$$

$$h_3=0.5mm,\ \tilde{h}_2=h_2/h_3,\ \tilde{h}_1=h_1/h_3,\ D_k=\frac{E_3h_3^2}{12(1-\upsilon_3^2)},\ K_o=\frac{-P_0h_3b^2}{D_k},\ K_t=\frac{-P_th_3b^2}{D_k}$$

The damping effects of the sandwich system are provided by the ER fluid in this study, and only the electric field dependence of ER fluid needed to consider based on the existing model of ER material. Therefore, the complex modulus of ER fluid can be simplified into the following equation,

Table 1 Comparison between published and proposed methods for the full coverage annular plate. Boundary condition: Clamped at inner edge and free at outer edge ($K_0 = 0$, $K_t = 0$)

Mode (n, m)	Natural frequency (Hz)		Modal loss factor (%)	
	Proposed	Roy and Ganesan (1993)	Proposed	Roy and Ganesan (1993)
(0,0)	74.44	74.38	11.28	11.27
(0,1)	73.00	73.08	9.542	9.576
(0,2)	96.20	96.38	10.16	10.21
(0,3)	144.0	142.8	12.10	12.12
(0,4)	205.2	203.7	11.70	11.77

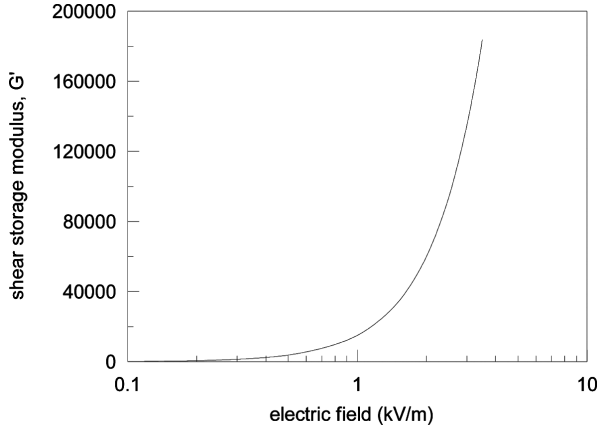

Fig. 3 Shear storage modulus dependence on electric fields for the ER material

which was experimentally measured by Don (1993)

$$G_2(E_*) = G' + jG'' \tag{17}$$

where G' is the shear storage modulus, G'' is the loss modulus ($G'' \approx 6900$), E_* is the applied electric field in kV/mm, and $j = \sqrt{-1}$, respectively. And, the variations of the shear storage modulus with different applied electric fields are shown in Fig. 3. In the following discussions, ω^* is the natural frequency of the sandwich annular plate with the parameters $\tilde{a}$=0.1, $\tilde{h}$=0.5 , h_3=0.5 mm, K_o=K_t=0 , and subjected to electric filed E_* = 0.5 kV/mm. In addition, the boundary conditions are clamped at inner edge and free at outer edge and the number of elements in the r-direction is taken to be 16.

The stability-instability boundaries are calculated and obtained by the first approximation in Eq. (16). The effects of applying electric fields on the primary instability regions for the sandwich annular plate system are shown in Fig. 4. The primary instability region for the sandwich system will shift to the positive $\Theta/2\omega^*$ direction and also shift to the negative K_t direction with increasing of applying electric fields. It is because that the applying electric field will change the material property of ER fluid core and also increase the stiffness of the sandwich system. Additionally, it can be observed that the tendency is similar for different thickness of ER core layer as shown in Figs. 4(a) and (b). Figs. 5(a) and (b) show the effects of ER core thickness on the primary instability regions for the sandwich annular plate system with applying electric fields E_* = 0.5 and E_* = 1.5 kV/

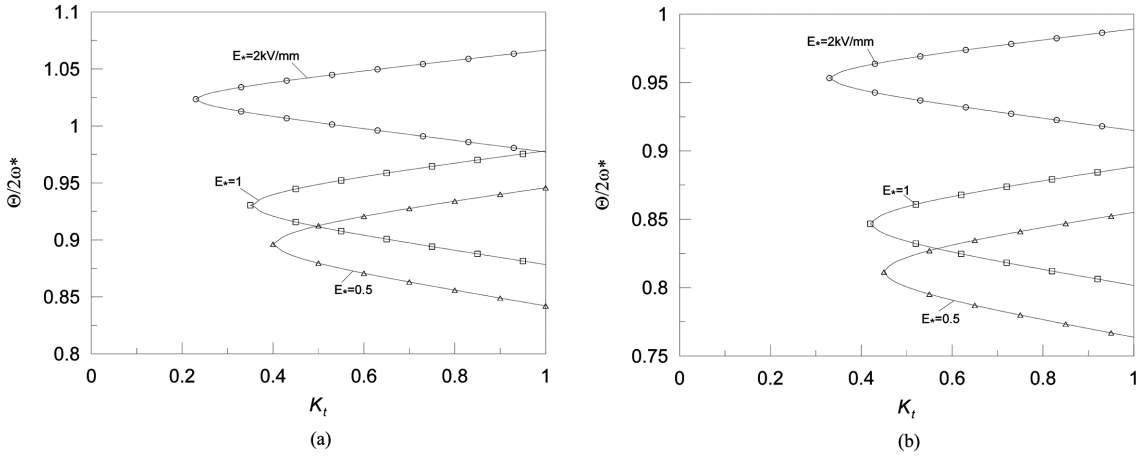

Fig. 4 Effects of applying electric fields on the primary instability regions. (a) $\tilde{h}_2$=0.5 and (b) $\tilde{h}_2$=1.0 ($\tilde{a}$=0.1, $\tilde{h}$=0.1 , K_o=1)

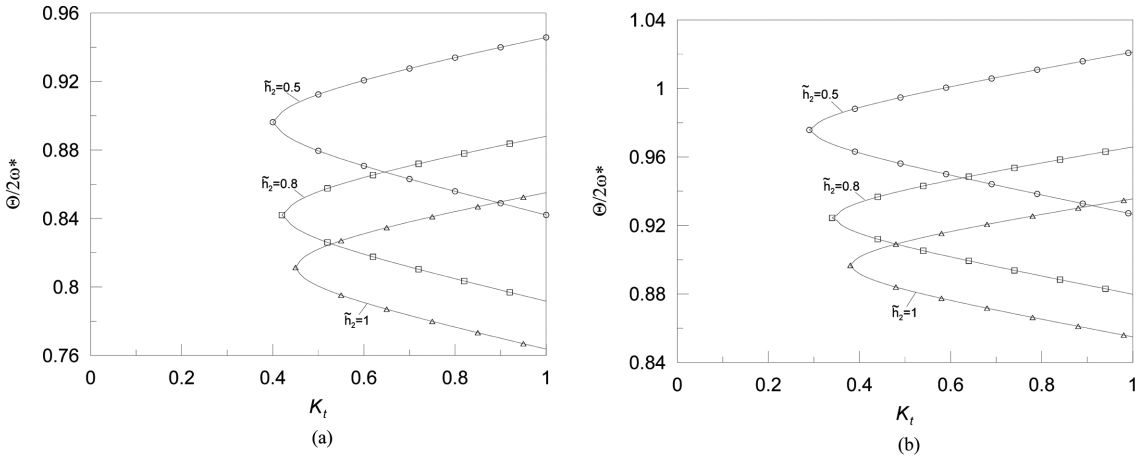

Fig. 5 Effects of ER core layer thickness on the primary instability regions. (a) E_*=0.5 kV/mm and (b) E_*=1.5 kV/mm ($\tilde{a}$=0.1, $\tilde{h}_1$=0.1, K_o=1)

mm. With increasing of ER core thickness, the primary instability region for the sandwich system will move towards the negative $\Theta/2\omega^*$ direction and also shift to the postive K_t direction. And, the instability regions of the sandwich system will have larger disturbance frequency with the higher applying electric fields from the numerical results. The effects of constraining layer thickness on the primary instability regions with applying electric fields E_* = 0.5 and E_* = 1.5 kV/mm are plotted in Figs. 6(a) and (b), respectively. The results show that the damping effects will increase with the increasing of the constraining layer thickness. It is because that the larger the constraining layer thickness is, the higher shear deformation in the sandwich system. In addition, the variation tendency for different applying electric fields shows the similar results.

The effects of the static load factor K_0 with various applying electric fields are plotted in Fig. 7. The instability regions of the sandwich system will move towards the positive $\Theta/2\omega$* direction and reduce with increasing of applying electric fields. The reason is the applying electric change the

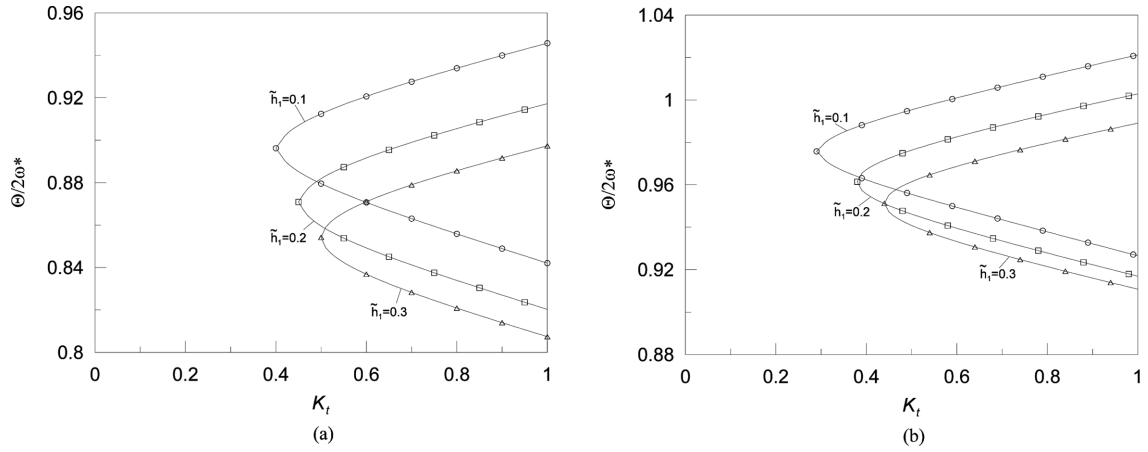

Fig. 6 Effects of constraining layer thickness on the primary instability regions. (a) E_*=0.5 kV/mm and (b) E_*= 1.5 kV/mm ($\tilde{a}$=0.1, $\tilde{h}_2$=0.5, K_o=1)

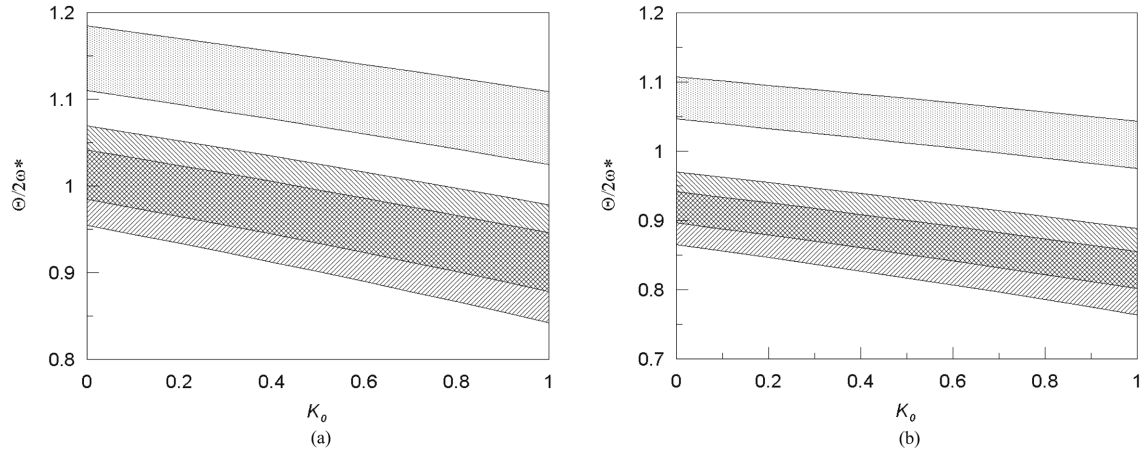

Fig. 7 Effects of static load parameter K_o on the primary instability regions with various applying electric fields. E_*=0.5 kV/mm: ▨E_*=1: ▧ E_*=2.5: ⬚ (a) $\tilde{h}_2$=0.5 and (b) $\tilde{h}_2$=1.0 ($\tilde{a}$=0.1, $\tilde{h}_1$=0.1, K_t = 1)

stiffness of the sandwich system. Moreover, the larger ER core layer thickness is, the smaller instability region of the system with the same applying electric fields will be. Fig. 8 shows the effects of the static load factor K_0 with various ER core layer thicknesses. The instability regions will shift to negative $\Theta/2\omega^*$ direction with increasing of ER core layer thickness. The reasons are due to the increment of stiffness for the sandwich annular plate system. For the different applying electric fields, the tendency is similar according to the figures. Finally, the effects of static load parameter K_o on the primary instability region with various inner radius ratios are presented in Fig. 9. It can be found that the inner radius will affect the position of the instability region of the sandwich plate system and cause instability regions move towards the positive $\Theta/2\omega^*$ direction. It is because that the inner radius ratio $\tilde{a}$ will change the relative stiffness of the system and can be utilized to control the instability regions of the sandwich annular plate system.

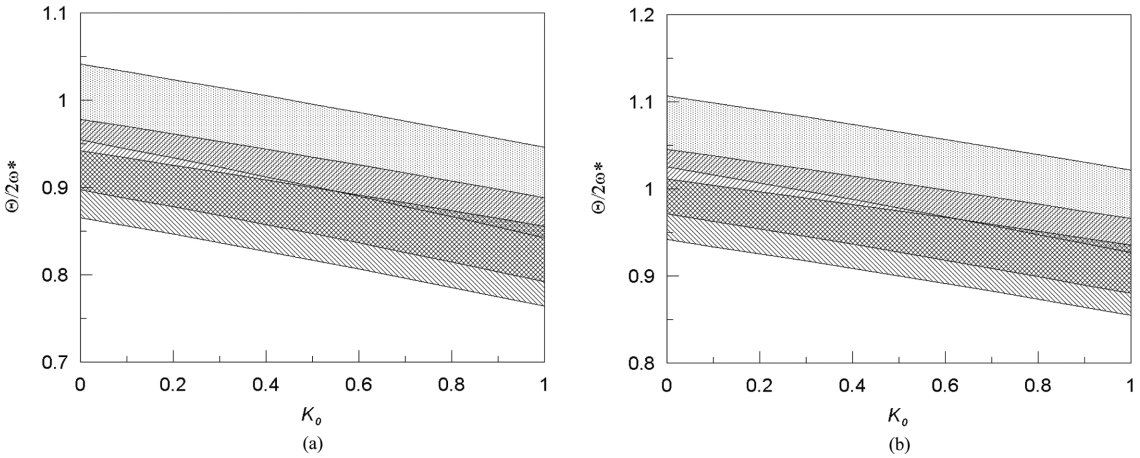

Fig. 8 Effects of static load parameter K_o on the primary instability regions with various ER core layer thickness. $\tilde{h}_2$=0.5 : $\tilde{h}_2$=0.8 : $\tilde{h}_2$=1.0 : (a) E_*=0.5 kV/mm and (b) E_*=1.5 kV/mm ($\tilde{a}$=0.1, $\tilde{h}_1$=0.1 , K_t=1)

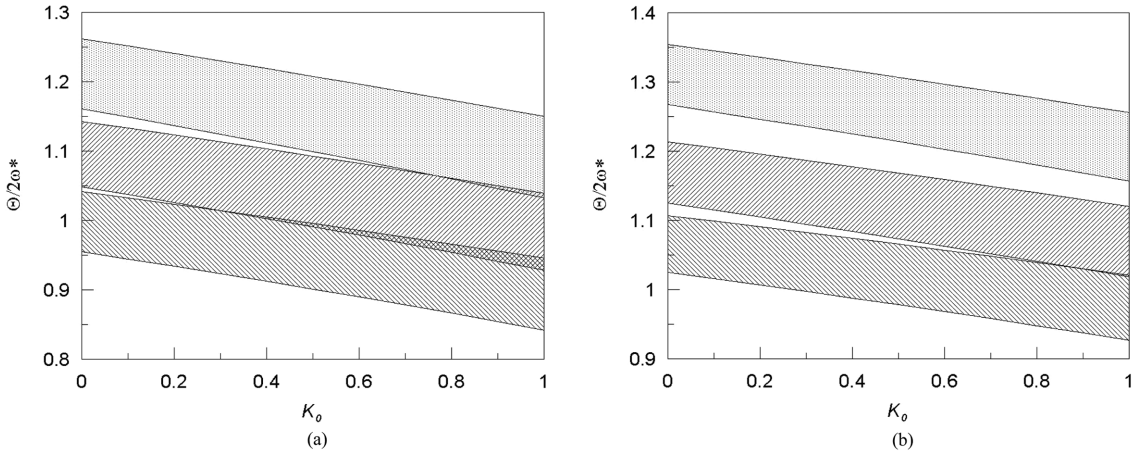

Fig. 9 Effects of static load parameter K_o on the primary instability regions with various inner radius ratios. $\tilde{a}$=0.1: $\tilde{a}$=0.15 : $\tilde{a}$=0.2 : (a) E_*=0.5 kV/mm and (b) E_*=1.5 kV/mm ($\tilde{h}_1$=0.1, $\tilde{h}_2$=0.5 , K_o=1)

4. Conclusions

The parametric resonance of the axisymmetric sandwich annular plate with an ER fluid core layer and constrained layer are studied in this paper. By using the discrete layer annular finite element method and the harmonic balance method, the boundaries of the instability regions of the sandwich annular plate are calculated and obtained. According to the numerical results, the following conclusions can be drawn:

1. According to the numerical results, the applying electric field, the ER fluid layer, the constraining layer, and some designed parameters can utilized to change the stability characteristics and instability regions of sandwich annular plate system.
2. It can be observed that the applying electric fields E_* will change the stiffness of the annular

sandwich plate, and boundaries of the instability regions of the sandwich annular plate system can be changed when applying different electric fields.

3. The boundaries of the instability regions of the sandwich annular plate system will be changed and controlled with various thickness of the ER layer.
4. The ER materials, which can be changed by applying different electric fields, are shown to have significant effects on the instability regions of the sandwich system.

The present results hope to provide the basic information for practical applications. In addition, we also can design some active controllable and more stable mechanical devices according to the above results. Besides, the dynamic stability problems of sandwich shells and rotating annular plate with ER fluid core are also interesting topics to be studied.

References

Bolotin, V.V. (1964), *The dynamic stability of elastic system*, Holden-Day San Francisco.

Chen Y.R. and Chen L.W. (2004), "Axisymmetric parametric resonance of polar orthotropic sandwich annular plates", *Compos. Struct*., **65**(3-4), 269-277.

Chen, L.W. and Hwang, J.R. (1988), "Axisymmetric dynamic stability of polar orthotropic thick circular plates", *J. Sound Vib*., **125**(3), 555-563.

Chen, L.W. and Hwang, J.R. (1988), "Axisymmetric dynamic stability of transverse isotropic Mindlin circular plates", *J. Sound Vib*., **121**(2), 307-315.

Coulter, J.P. (1993), "Engineering application of electrorheological materials", *J. Intell. Mater. Syst. Struct*., **4**(2), 248-259

Don, D.L. (1993), *An investigation of electrorheological material adoptive structure*, Master's Thesis Lehigh University Bethlehem Pennsylvania.

Evan-Iwanowski, R.M. (1976), *Resonance oscillations in mechanical systems*, Amsterdam Elsevier.

Ilyasov, M.H. and Akoz, A.Y. (2000), "The vibration and dynamic stability of viscoelastic plates", *Int. J. Eng. Sci*., **38**(6), 695-714.

Kang, Y.K., Kim, J. and Choi, S.B. (2001), "Passive and active damping characteristics of smart electro-rheological composite beams", *Smart Mater. Struct*., **10**(4), 724-729.

Oyadiji, S.O. (1996), "Application of electro-rheological fluids for constrained layer damping treatment of structures", *J. Intell. Mater. Syst. Struct*., 7, 541-549.

Roy, P.K. and Ganesan, N. (1993), "A vibration and damping analysis of circular plates with constrained damping layer treatment", *Comput. Struct*., **49**(2), 269-274.

Stevens, K.K. (1966), "On the parametric excitation of a viscoelastic column", A.I.A.A. J., **4**(12), 2111-2116.

Stevens, K.K. (1969), "Transverse vibration of a viscoelastic column with initial curvature under periodic axial load", *J. Appl. Mech - T ASME*., **36**(4), 814-818.

Tani, J. and Doki, H. (1982), "Dynamic stability of orthotropic annular plates under pulsating redial loads", *J. Acoust. Soc. Am*., **69**, 1688-1694.

Tani, J. and Nakamura, T. (1980), "Dynamic stability of annular plates under pulsating torsion", *J. Appl. Mech - T ASME*., **47**(3), 595-600.

Touati, D. and Cederbaum, G. (1994), "Dynamic stability of nonlinear viscoelastic plates", *Int. J. Solids Struct*., **31**(17), 2367-2376.

Weiss, K.D., Coulter, J.P. and Carlson, J.D. (1993) "Material aspects of electro-rheological system", *J. Intell. Mater. Syst. Struct*., **4**(1), 13-34

Yalcintas, M. and Coulter, J.P. (1995), "Analytical Modeling of Electrorheological Material Based Adaptive Beams", *J. Intell. Mater. Syst. Struct*., **6(4)**, 488-497.

Yalcintas, M. and Coulter, J.P. (1995), "Electrorheological Material Based Adaptive Beams Subjected to Various Boundary Conditions", *J. Intell. Mater. Syst. Struct*., **6**(5), 700-717.

FC

Appendix

1. $H_{1,i}(z)=\begin{bmatrix}(\frac{1}{2}-\frac{z}{h_i}) & (\frac{1}{2}+\frac{z}{h_i}) & 0\\ 0 & 0 & 1\end{bmatrix}$

2. $q_i^e=\left\{U_i^A \quad V_i^A \quad U_{i+1}^A \quad V_{i+1}^A \quad W^A \quad \Theta^A \quad U_i^B \quad V_i^B \quad U_{i+1}^B \quad V_{i+1}^B \quad W^B \quad \Theta^B\right\}^T$

3. $H_2(r)=\begin{bmatrix}\phi_u^A & 0 & 0 & 0 & \phi_u^B & 0 & 0 & 0\\ 0 & \phi_u^A & 0 & 0 & 0 & \phi_u^B & 0 & 0\\ 0 & 0 & \phi_w^A & \phi_\Theta^A & 0 & 0 & \phi_w^B & \phi_\Theta^B\end{bmatrix}$

where

$\phi_u^A=(1-\xi)$, $\phi_u^B=\xi$, $\phi_w^A=(1-3\xi^2+2\xi^3)$, $\phi_w^B=(3\xi^2-2\xi^3)$, $\phi_\Theta^A=(\xi-2\xi^2+\xi^3)$,

$\phi_\Theta^B=(-\xi^2+\xi^3)$, $\xi=\dfrac{r-r_i}{r_0-r_i}$

4. $\begin{bmatrix}\dfrac{\partial}{\partial r} & 0\\ \dfrac{1}{r} & 0\\ \dfrac{\partial}{\partial z} & \dfrac{\partial}{\partial z}\end{bmatrix}$

5. $C_i=\begin{bmatrix}C_{11,i} & C_{12,i} & 0\\ C_{21,i} & C_{22,i} & 0\\ 0 & 0 & C_{44,i}\end{bmatrix}$

for the isotropic material, $C_{11,i}=C_{22,i}=\dfrac{E_i}{1-\upsilon_i^2}$, $C_{12,i}=C_{21,i}=\dfrac{\upsilon_i E_i}{1-\upsilon_i^2}$, $C_{44,i}=\kappa^2\dfrac{E_i}{1-\upsilon_i^2}$, respectively. In the above equations, E_i is the Young's modulus, υ_i is the Poisson ration, and κ^2 is the shear correction factor. Besides, for layer 1 and layer 3, the shear correction factor is taken to be $\pi^2/12$, while to be 1 for layer 2.

6. $\overline{\sigma}_i=\begin{Bmatrix}\overline{\sigma}_{r,i}\\ \overline{\sigma}_{\theta,i}\\ \overline{\tau}_{rz,i}\end{Bmatrix}=C_iD(H_{1,i}H_2)\overline{\mathrm{U}}_i^e$, $\quad \overline{\varepsilon}_i=\begin{Bmatrix}\frac{1}{2}(\frac{\partial u_i}{\partial r})^2+\frac{1}{2}(\frac{\partial w_i}{\partial r})^2\\ \frac{1}{2}(\frac{u_i}{r})^2\\ \frac{\partial u_i}{\partial r}\frac{\partial u_i}{\partial z}\end{Bmatrix}$

in which, $\overline{\mathrm{U}}_i^e$ is the equilibrium nodal displacement vector of the annular element for *i*th layer.

$$\mathrm{M}_i^e = \int_V (DH_{1,i}H_2)^{\mathrm{T}} C_i^{\mathrm{T}} (DH_{1,i}H_2) dV$$

$$\mathrm{K}_i^e = \int_V \rho_i (H_{1,i}H_2)^{\mathrm{T}} (H_{1,i}H_2) dV$$

7.
$$\mathrm{G}_i^e = 2\int_V [(D_1H_4H_{1,i}H_2)^T \hat{\sigma}_i^e (D_2H_4H_{1,i}H_2) + (D_1H_5H_{1,i}H_2)^T \hat{\sigma}_i^e (D_2H_5H_{1,i}H_2)$$
$$+ \frac{1}{2}(D_3H_5H_{1,i}H_2)^T \hat{\sigma}_i^e (D_3H_5H_{1,i}H_2)] dV$$

in which

$$D_1 = \begin{Bmatrix} \frac{1}{2}\frac{\partial}{\partial r} \\ 0 \\ \frac{\partial}{\partial r} \end{Bmatrix}, \quad D_2 = \begin{Bmatrix} \frac{\partial}{\partial r} \\ 0 \\ \frac{\partial}{\partial z} \end{Bmatrix}, \quad D_3 = \begin{Bmatrix} 0 \\ \frac{1}{r} \\ 0 \end{Bmatrix}, \quad \hat{\sigma}_i^e = \begin{bmatrix} \overline{\sigma}_{r,i}^e & 0 & 0 \\ 0 & \overline{\sigma}_{\theta,i}^e & 0 \\ 0 & 0 & \overline{\tau}_{rz,i}^e \end{bmatrix}$$

$$H_4 = [1 \quad 0], \quad H_5 = [0 \quad 1]$$